An Embedded Boundary Method for Solving the Stress-Balance Equation of Ice Sheet Dynamics

Will Thacher, Hans Johansen, and Daniel Martin

Applied Numerical Algorithms Group, Lawrence Berkeley National Laboratory

MOTIVATION

As global temperatures continue to climb, Antarctica and other large ice sheets become increasingly vulnerable to loss of mass, which can contribute significantly to global sea level rise. This research builds on the **BISICLES** model, (Cornford and Martin, 2013) a state-of-the-art tool for simulating large-scale dynamics of ice sheets and making quantitative predictions about future contributions to sea level rise.

A region of particular importance in ice sheet physics is the near the ***grounding line***, which demarcates ice that sits on bedrock below sea level and ice that floats in the sea. This is a region of dynamic activity that is highly consequential for ice sheet mass loss.

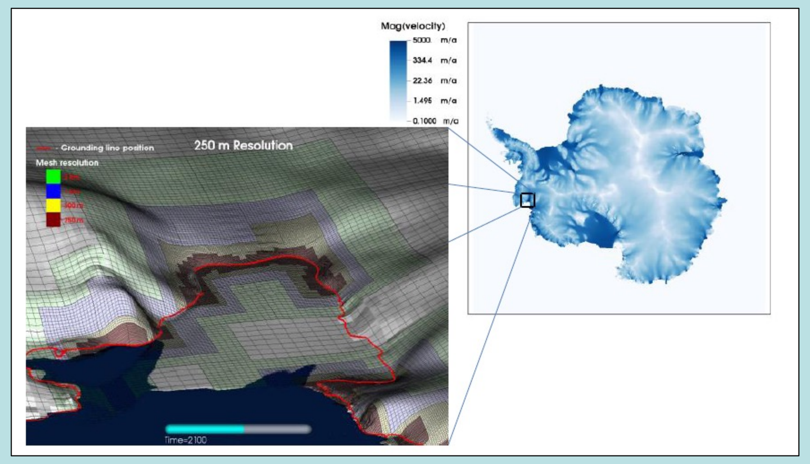

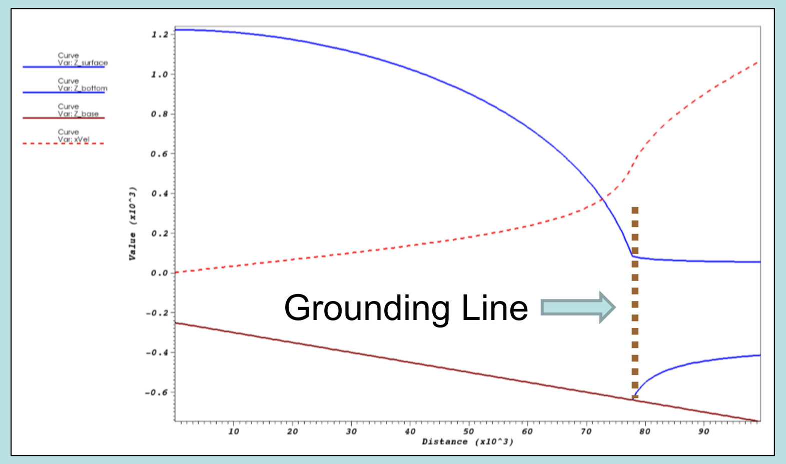

Left: BISICLES simulation of Antarctic ice sheet with grounding line marked in red. **Right:** 1D profile of ice sheet surface at grounding line. Note the kink in the ice surface at the grounding line.

As ice lifts off bedrock and flows into the sea, it can no longer balance the stress of gravity through friction with the ground. This abrupt change in the stress-balance equation at the grounding line can result in a loss of numerical accuracy if not properly addressed. The guiding idea for this method is to treat the grounding line as an interface between two “phases” of ice (grounded and floating) which are coupled by jump conditions at the interface. This problem is well suited for an ***embedded boundary (EB)*** method, in which the grounding line is represented as a curve intersecting a uniform Cartesian mesh, creating “cut cells” where the finite-volume discretization of the stress balance equation must be appropriately modified.

GOVERNING EQUATIONS

We consider the “Shallow-Shelf” approximation (MacAyeal, 1996) to the full Stokes equations, which takes advantage of the fact that ice sheets have a large aspect ratio, or ratio of horizontal to vertical length scale. Ice is treated as a shear-thinning, non-Newtonian fluid that can deform or slide on top of bedrock to balance a gravity-driven stress. This approximation reduces the constitutive equation to a set of 2D coupled non-linear elliptic equations to be solved for the x and y components of the velocity field:

$$-\beta\boldsymbol{u} + \nabla\cdot(H\mu\boldsymbol{F}(\boldsymbol{u})) = \rho g H\,\nabla s$$

where H is the ice thickness, $\boldsymbol{u} = (u, v)$ is the velocity field at the base of the ice sheet, β is the nonlinear frictional sliding coefficient, μ is the nonlinear viscosity, s is the surface height of the ice, ρ is the density of ice and g is gravitational acceleration. $\boldsymbol{F}(\boldsymbol{u})$ is the stress tensor, which depends on various partial derivatives of $\boldsymbol{u}$.

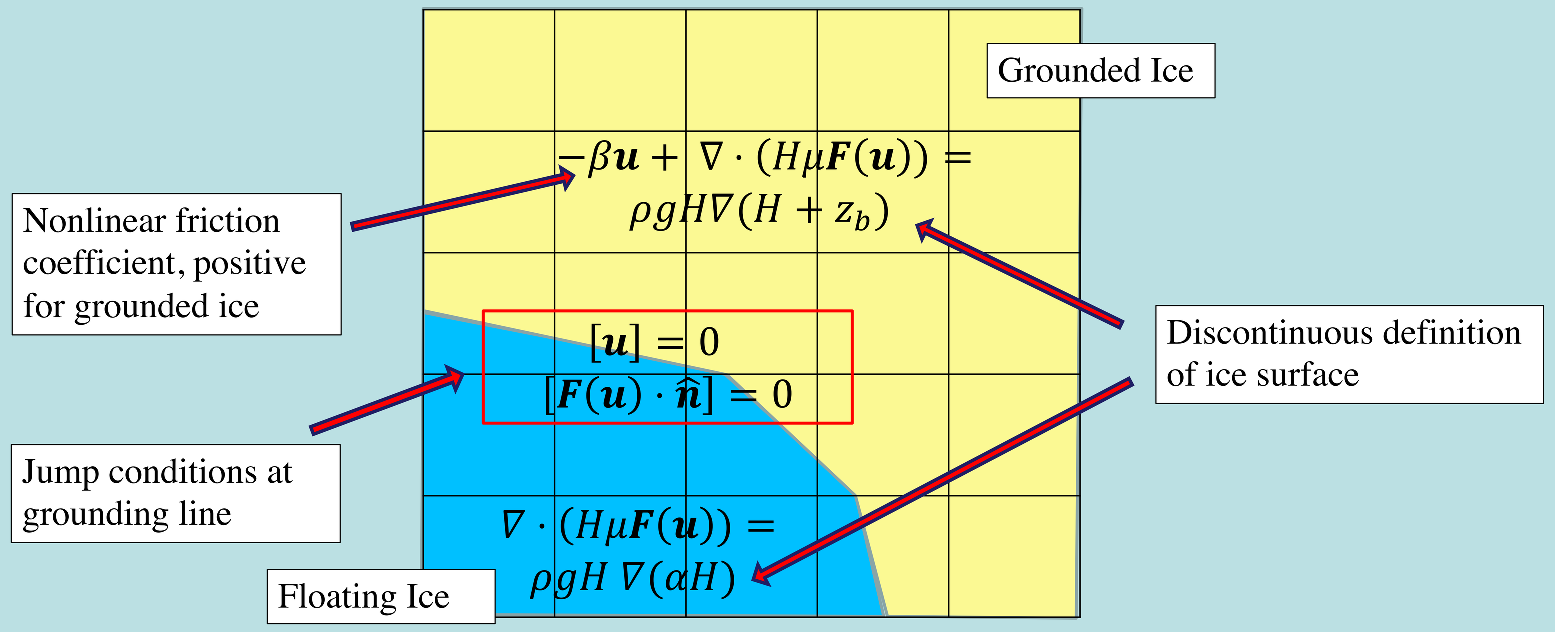

This PDE has variable coefficients that are discontinuous at the grounding line: the sliding coefficient is positive for grounded ice and zero for floating ice, ice thickness may have a second order discontinuity, the viscosity is not necessarily smooth, and the right-hand-side driving stress is discontinuous as the gradient of the ice surface abruptly jumps.

EMBEDDED BOUNDARY DISCRETIZATION

We solve the stress balance equation using a conservative finite-volume scheme, meaning the stress balance equation is integrated over each discrete full and cut cell. We apply Gauss’ theorem to the flux divergence term and integrate the flux over cell faces, including the EB.

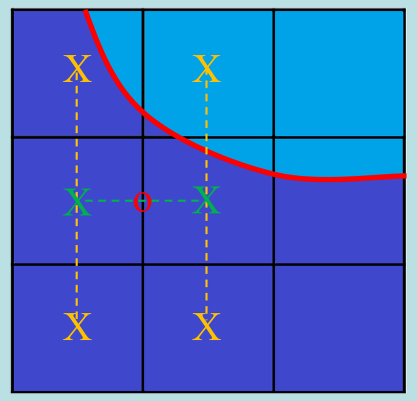

Left: EB intersecting Cartesian mesh. Finite difference schemes (in gold) that reach across the grounding line violate smoothness requirements and are invalid. **Right:** Cut cell containing grounded and floating volumes with geometric quantities notated – V represents a volume and A represents an area over which the flux is integrated.

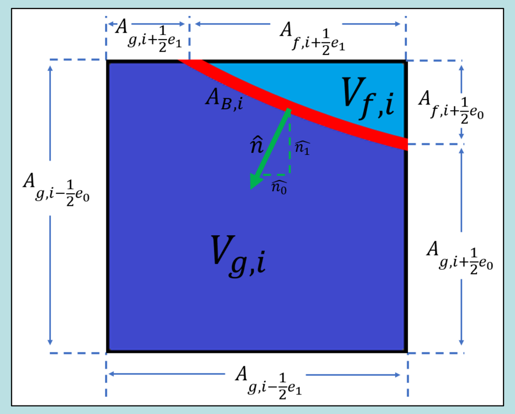

The basic strategy is to write integrals in terms of Taylor expansions in each variable, and then directly compute the coefficients $c_\phi^{\boldsymbol{p}}$ in the Taylor expansions by interpolating discrete values of each variable. For example, for the x-component of the basal traction term, we have:

$$\int_V \beta\, u\, dV = \int_V \sum_{|\boldsymbol{p}|\le Q} c_\beta^{\boldsymbol{p}} x^{\boldsymbol{p}} \sum_{|\boldsymbol{q}|\le Q} c_u^{\boldsymbol{q}} x^{\boldsymbol{q}} + O(h^{Q+1})\, dV$$

$$= \underbrace{[\beta_1, \beta_2 \dots \beta_n]}_{\text{Local values of }\beta}\underbrace{(\boldsymbol{M}_\beta^+)^T}_{\text{Interpolation Matrix}} \underbrace{\begin{pmatrix} \int_V \boldsymbol{x}^{\boldsymbol{p_1}+\boldsymbol{q_1}}\, dV & \cdots & \int_V \boldsymbol{x}^{\boldsymbol{p_1}+\boldsymbol{q_m}}\, dV \\ \vdots & \ddots & \vdots \\ \int_V \boldsymbol{x}^{\boldsymbol{p_m}+\boldsymbol{q_1}}\, dV & \cdots & \int_V \boldsymbol{x}^{\boldsymbol{p_m}+\boldsymbol{q_m}}\, dV \end{pmatrix}}_{\text{Integrals of polynomial terms}} \underbrace{\boldsymbol{M}_u^+}_{\text{Interpolation Matrix}} \underbrace{[u_1, u_2 \dots u_n]^T}_{\text{Local values of }u} + \underbrace{O(h^{Q+1})}_{\text{Truncation Error}}$$

We can multiply the four matrices on the left together to obtain a row vector of weights for local values of the dependent variable u , i.e., a stencil. We can obtain similar expressions for the right-hand-side and flux divergence term. This formulation works in both full and cut cells.

$\boldsymbol{M}_\beta$ and $\boldsymbol{M}_u$ are Vandermonde-type matrices that interpolate local values of their respective fields. If the neighborhood of values is chosen correctly, we can solve a small overdetermined linear system for the Taylor polynomial coefficients: $M_\phi\, c_\phi^{\boldsymbol{p}} = [\phi_1 \dots \phi_n]^T$. Jump conditions on $\boldsymbol{u}$ and $\boldsymbol{F}(\boldsymbol{u})$ can be written in terms of the same Taylor coefficients, so we force the Taylor polynomial to obey jump conditions by adding jump equations to the interpolation matrix.

INTERFACE RECONSTRUCTION

For cut cell stencils, the three matrices in the middle of the stencil expression above rely on geometric information that involves the position and shape of the grounding line. The grounding line is the zero contour of the “thickness above flotation” field $H_f = H + \frac{\rho_w}{\rho} z_b$, where z_b is the bedrock height. Our reconstruction algorithm must respect potential second-order discontinuities in the ice thickness field.

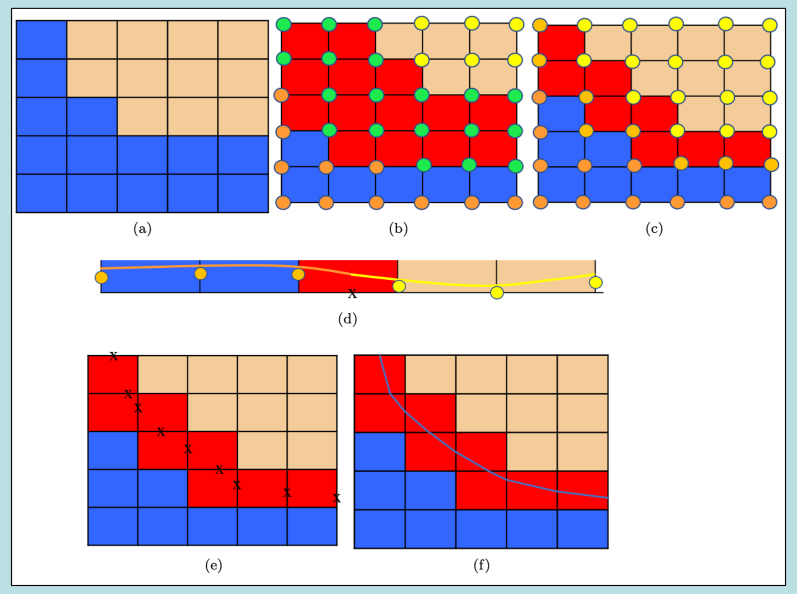

Left: EB Reconstruction from cell-averaged H_f values. Blue cells are floating, tan cells are grounded, and red cells are iteratively reduced from a potential to final set of cut cells. Nodal point values of H_f (in orange and yellow) are used in a root-finding algorithm to locate intersections of the EB with the Cartesian grid. Splines are fit through the intersections to obtain more accurate geometric information.

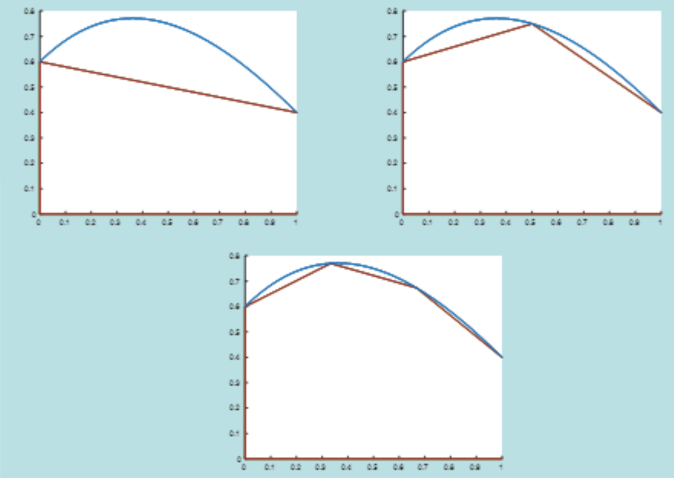

Right: Integrals of polynomial terms over cut cell fractions are calculated using Green’s Theorem over increasingly refined polygons fit to the splines. Convergence is accelerated using Richardson extrapolation. Errors in geometric quantities contribute to truncation error, so more accurate geometric information is required for a higher order discretization.

RESULTS

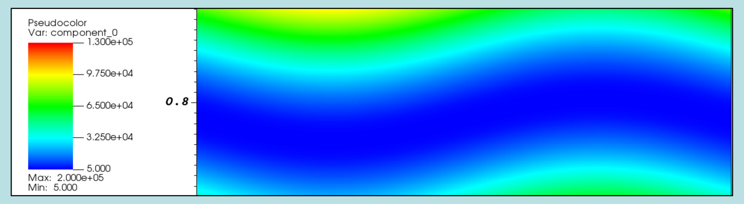

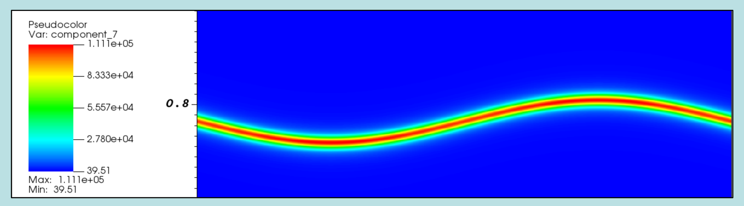

Left: Sinusoidally varying basal friction field creates an ice stream. **Right:** Resulting velocity magnitude.

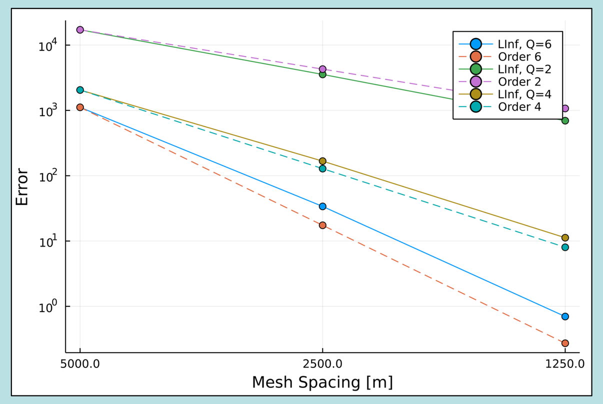

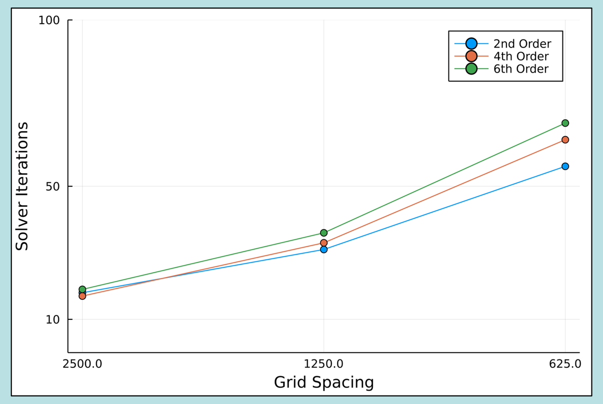

Left: 2[nd], 4[th], and 6[th] order convergence of error in x-component of velocity for ice stream test linearized around constant μ. **Right:** Number of GMRES iterations required for linear solve changes only slightly with order of discretization, indicating robustness of discretization scheme.

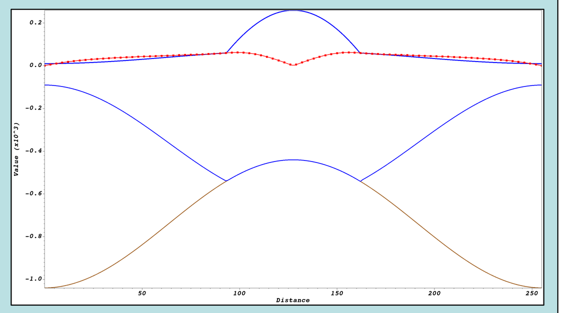

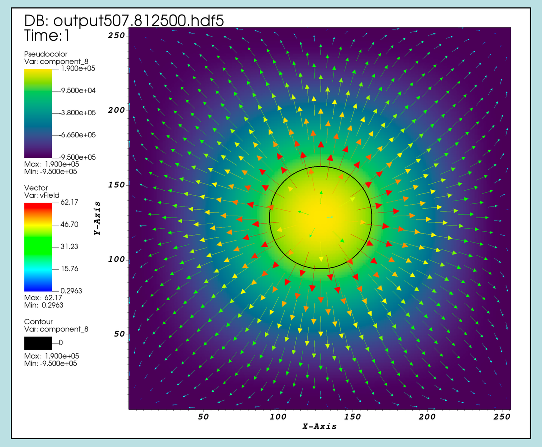

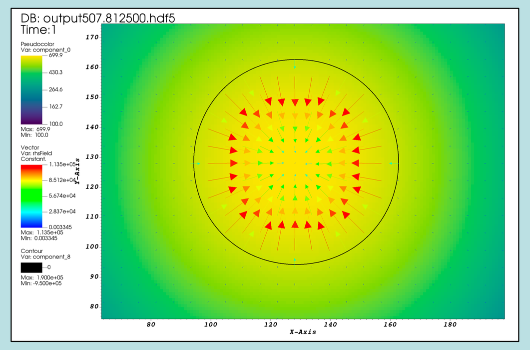

Left: Cross-section of basal topography, upper and lower surface of ice, and velocity magnitude for “ice rise” experiment. **Middle:** Velocity field. Colormap is of H_f field, and black circle marks grounded portion of ice sheet. **Right:** Grounded detail of RHS driving stress with colormap of ice thickness.

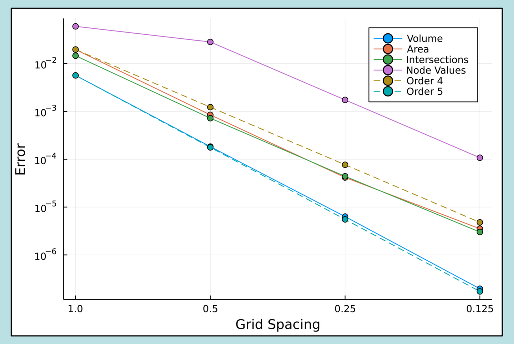

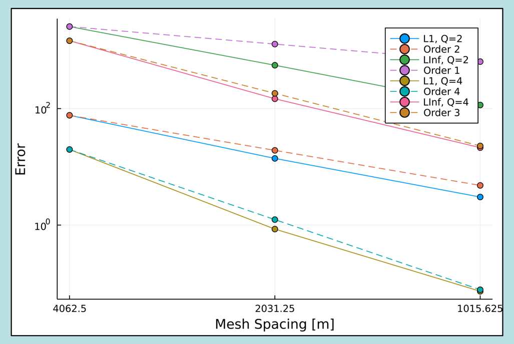

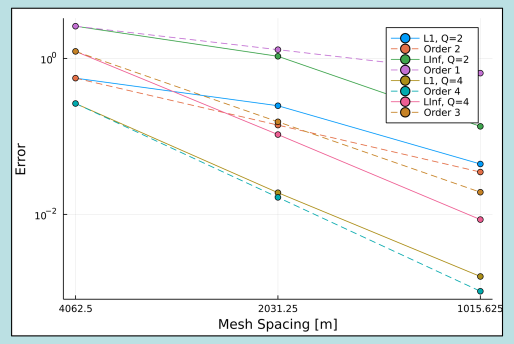

Left: Interface reconstruction error is 5[th] order accurate, meaning it does not infect truncation error. **Middle:** 2[nd] and 4[th] order convergence of error in x-component of RHS. **Right:** 2[nd] and 4[th] order convergence of error in x-component of velocity. Max norm error can be one order of accuracy lower due to error in and near EB cells; however, the set of EB cells is of O(1/h), so the L1 error is order Q.

CONCLUSIONS/FUTURE WORK

We have developed and verified a novel embedded boundary discretization scheme for solving the Shallow-Shelf equations. Our discretization scheme is higher order accurate and generally applies to elliptic equations with variable coefficients that are discontinuous at an interface; the stress-balance equation is a challenging example in this class of equations.

The interface reconstruction scheme is local, highly parallelizable, and computationally inexpensive. This is critical because the interface will move and morph in time and needs to be rebuilt every timestep.

There is much future work to be done: incorporating this scheme with the parallel, adaptive mesh refinement techniques that are currently used in BISICLES, building a robust geometric multigrid solver, and testing the method on realistic ice sheet problems. There is a great degree of flexibility in constructing valid (in terms of truncation error) interpolation matrices that define the stencils, which can be exploited to construct operators that are easier to invert.

Acknowledgements: This material is based upon work supported by the U.S. Department of Energy, Office of Science, Advanced Scientific Computing Research, under contract number DE-AC02-05CH11231.